

Dalton Transactions

An international journal of inorganic chemistry

Accepted Manuscript

This article can be cited before page numbers have been issued, to do this please use: A. Bhanja, E. Moreno Pineda, R. Herchel, W. Wernsdorfer and D. Ray, *Dalton Trans.*, 2020, DOI: 10.1039/D0DT01675F.



This is an Accepted Manuscript, which has been through the Royal Society of Chemistry peer review process and has been accepted for publication.

Accepted Manuscripts are published online shortly after acceptance, before technical editing, formatting and proof reading. Using this free service, authors can make their results available to the community, in citable form, before we publish the edited article. We will replace this Accepted Manuscript with the edited and formatted Advance Article as soon as it is available.

You can find more information about Accepted Manuscripts in the [Information for Authors](#).

Please note that technical editing may introduce minor changes to the text and/or graphics, which may alter content. The journal's standard [Terms & Conditions](#) and the [Ethical guidelines](#) still apply. In no event shall the Royal Society of Chemistry be held responsible for any errors or omissions in this Accepted Manuscript or any consequences arising from the use of any information it contains.

ARTICLE

Self-Assembled Octanuclear [Ni₅Ln₃] (Ln = Dy, Tb and Ho) Complexes: Synthesis, Coordination Induced Ligand Hydrolysis, Structure and Magnetism

Received 00th January 20xx,
Accepted 00th January 20xx

DOI: 10.1039/x0xx00000x

Avik Bhanja,^a Eufemio Moreno-Pineda^{b,c}, Radovan Herchel^d, Wolfgang Wernsdorfer^{b,e,f}, Debashis Ray^{*a}

The variable coordination behavior of 2-[[[(2-hydroxy-3-methoxybenzyl)imino]methyl]-6-methoxyphenol (H₂L) and its hydrolyzed congener towards NiCl₂·6H₂O and Ln^{III} nitrate salts provide a family of coordination aggregates containing a [Ni₅Ln₃] octanuclear core structure. Room temperature reactions in MeOH–CHCl₃ medium and in the presence of NEt₃ yield isostructural [Ni₅Ln₃(L)₄(μ-OH)₂(μ₃-OH)₆(*o*-val)₂(H₂O)₆]NO₃·7H₂O (Ln = Dy³⁺ (**1**), Tb³⁺ (**2**), and Ho³⁺ (**3**); *o*-val = *o*-vanillin) heterometallic complexes. All the three complexes hold an octanuclear fused partial hexacubane topology from the utilization of phenolate-based ligand anions, clipping five 3d and three 4f ions. Direct current magnetic susceptibility measurements showed an upsurge at low temperature for complex **1** and **2**, indicative of ferromagnetic interactions while antiferromagnetic exchange interaction predominates for complex **3**. AC magnetic susceptibility measurements were not able to show any slow relaxation property to the magnetization. CASSCF calculations for complex **1** indicates all three Dy³⁺ centres have anisotropic axes but the relative orientation of the magnetic axes reduce the probability of this molecule to behave like a SMM which further established by the POLY_ANISO calculations.

Introduction

In recent years the synthesis and characterization of multinuclear coordination aggregates bearing variable number of 3d and 4f ions in a single entity have attracted substantial consideration to fulfil the synthetic challenges leading to new avenues of reactions, aesthetically pleasing structures, and possibility of showing interesting molecule-based magnetic behaviour such as SMMs.¹ Use of phenol-based and imine nitrogen bearing ligand system for such aggregates of 3d–4f ions, showing varying coordination modes, has attracted enormous attention for their prospect in the possible applications in high-density information storage², quantum computing³, and molecular spintronics.⁴ Such molecular aggregates are designed and synthesized with a clear intention of achieving high ground state spin (*S*) values so that they can have high energy barrier (*U_{eff}*) to function as a new member of

the SMM family. But having high spin state or large *U_{eff}* barrier is not the sole criteria for achieving SMM property⁵; the magnetic anisotropy of an exchange-coupled system is equally important which again depends on the individual anisotropy of the metal ions and on the relative orientation of the local axes.⁶ Thus substantial effort is particularly given to Tb³⁺ (⁷F₆), Dy³⁺ (⁶H_{15/2}) and Ho³⁺ (⁵H₈) ions for constructing SMMs containing 3d–4f ions. Such compounds are expected to preserve the magnetic state for a long time interval even after removal of external magnetic fields, by suppression of ground state quantum tunnelling of magnetization (QTM).⁷ The Lewis acidic nature of 4f ions also helps in, to become bound water molecules acidic in nature and susceptible to controlled hydrolysis, resulted hydroxido supported growth of cluster-type magnetic cores.⁸ In this respect the ligand design is crucial which can simultaneously bind both the 3d and 4f metal ions within its chelating pockets; influencing both the effective energy barriers (*U_{eff}*) and magnetic blocking temperature (*T_B*). Incorporation of 3d ions in the aggregates, results in effective exchange coupling which stabilizes the bistable ground state and suppresses QTM.⁹

^a Department of Chemistry, Indian Institute of Technology, Kharagpur 721302, India

^b Institute of Nanotechnology (INT), Karlsruhe Institute of Technology (KIT), Hermann-von-Helmholtz-Platz 1, D-76344 Eggenstein-Leopoldshafen, Germany.

^c Depto. de Química-Física, Escuela de Química, Facultad de Ciencias Naturales, Exactas y Tecnología, Universidad de Panamá, Panamá, Panamá.

^d Department of Inorganic Chemistry, Faculty of Science, Palacky University, 17. listopadu 12, CZ-771 46 Olomouc, Czech Republic

^e Physikalisches Institut, Karlsruhe Institute of Technology, D-76131 Karlsruhe, Germany.

^f CNRS, Institut Néel, F-38042 Grenoble, France.

†Electronic Supplementary Information (ESI) available: FTIR, PXRD curves, crystal data, bond lengths and angles, TGA curves, ESI-MS spectrum, and CASSCF calculations. CCDC 1969074–1969076 contain the supplementary crystallographic data for this paper. See DOI: 10.1039/x0xx00000x

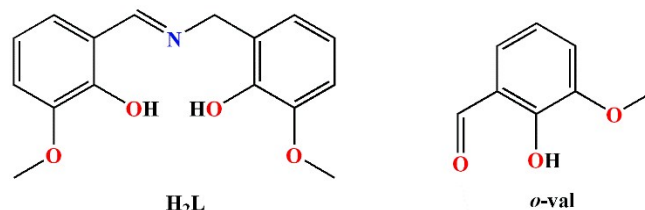


Fig. 1 Ligands utilized in the aggregate

Inclusion of V(III)¹⁰, Cr(III)¹¹, Mn(II/III/IV)¹², Fe(II/III)¹³, Co(II)¹⁴ and Cu(II)¹⁵ have thus been recognized for varying nuclearity and stimulating magnetic behaviour. Hence, the coordination ability of the imine nitrogen atoms for the 3d ions and –OMe group for the entrapment of bigger 4f ions can thus be explored in this background and this design strategy was fruitful in providing many Ni-4f complexes of varying nuclearity and unique structures.¹⁶

Herein, the ligand 2-[[2-hydroxy-3-methoxybenzyl)imino]methyl]-6-methoxyphenol (H₂L) (Chart 1) was examined for the first time to establish its simultaneous coordination ability to afford a new family of heterometallic octanuclear Ni₅Ln₃ complexes [Ni₅Ln₃(L)₄(μ-OH)₂(μ₃-OH)₆(o-val)₂(H₂O)₆]NO₃·7H₂O (Ln = Dy³⁺ (**1**), Tb³⁺ (**2**) and Ho³⁺ (**3**)). The anionic form of the Schiff base ligand H₂L was utilized to bring five Ni^{II} and three Ln^{III} within the same molecular aggregate. Until now, to the best of our knowledge, only one 3d-4f cluster bearing Ni₅Ln₃ magnetic core is reported.¹⁷ But in that case the cluster was built over carboxylate moiety whereas in this work, the entire cluster formed by the involvement of capping ligands and hydroxyl bridges formed from controlled hydrolysis of solvent molecules. Previously, we have shown that a central phenol based ligand system is useful for tetra- and pentanuclear aggregates, using two ligand anions.¹⁸ This prompted us to examine the reactivity pattern of H₂L toward multiple 3d and 4f ions for spontaneous self-assembly synthesis and most pertinent physical properties of the compounds.

Experimental Section

Starting materials and reagents

Solvents, starting materials and all other reagents used in this work were purified according to standard literature procedures.¹⁹ 3-methoxysalicylamine was synthesized following a reported procedure.²⁰ The following chemicals were used as received from commercial sources without further purification: NiCl₂·6H₂O and NEt₃ (S. D. Fine Chemicals, Mumbai, India), Dy(NO₃)₃·5H₂O, Ho(NO₃)₃·5H₂O and Tb(NO₃)₃·5H₂O (Alfa Aesar, India), o-vaniline (Spectrochem Pvt. Ltd. Mumbai). The ligand 2-[[2-hydroxy-3-methoxybenzyl)imino]methyl]-6-methoxyphenol (H₂L) was prepared by adapting a literature procedure.²¹

Synthesis of 2-[[2-hydroxy-3-methoxybenzyl)imino]methyl]-6-methoxyphenol (H₂L)

3-methoxy salicylamine hydrochloride salt (0.95 g, 5 mmol) was dissolved in 10 mL methanolic solution with the addition of solid K₂CO₃ (0.7 g, 5.1 mmol) under magnetic stirring. After 30 min of stirring a MeOH solution (20 mL) of o-vanillin (0.76 g, 5 mmol) was added drop-wise to the previously obtained clear solution and the whole mixture was refluxed for 4 h. A solid yellow product was isolated after complete removal of the solvent. Thorough and repeated washing with hexane gave a yellow solid powder which was then dried in vacuum over P₄O₁₀. Yield: 93% (1.33 g). ¹H NMR (400 MHz, CDCl₃): 8.4 (s, 1H), 7.3–6.9 (t, 2H), 6.9–6.8 (d, 4H), 4.8 (s, 2H), 3.8 (s, 6H). Selected FT-IR data

(KBr) cm⁻¹: 3431 (br), 2933 (m), 1648 (s), 1609 (m), 1527 (m), 1480 (s), 1334 (m), 1281 (s), 1243 (m), 1083 (s), 926 (w), 728 (m). Anal. Calcd for C₁₆H₁₇NO₄: C, 66.89; H, 5.96; N, 4.88. Found: C, 66.72; H, 5.84; N, 4.78.

General Procedure for Complexes 1–3

A MeOH solution (5 mL) of Ln(NO₃)₃·5H₂O (0.05 mmol) was added drop-wise into a stirred MeOH solution (10 mL) of H₂L (0.03 g, 0.1 mmol), followed by drop-wise addition of diluted NEt₃ (0.02 g, 0.2 mmol). After 1 h of stirring a MeOH solution (5 mL) of NiCl₂·6H₂O (0.024 g, 0.1 mmol) was added drop-wise to the previous yellow solution and the bright green reaction mixture thus obtained was stirred at room temperature for 12 h. The solution was filtered and left undisturbed for slow evaporation at room temperature. After one week, green crystalline powder was separated which was then recrystallized from MeOH–CHCl₃ (2:1) reaction mixture, resulting in green needle like crystals suitable for X-ray crystallographic analysis. The characterization data of the compounds and the quantity of the reactants used in each reaction are given below.

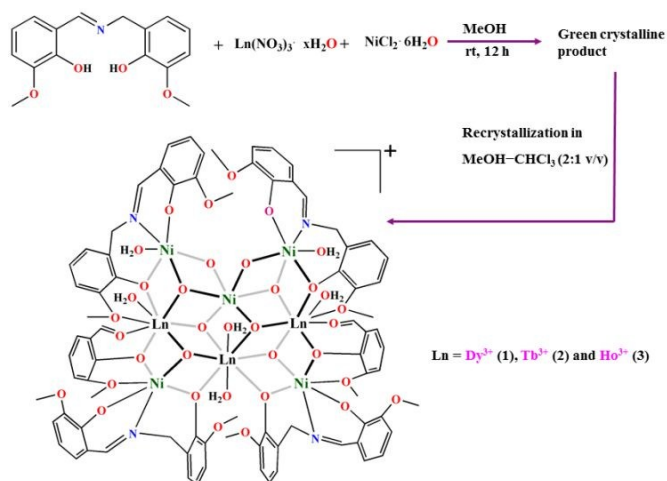
[Ni₅Dy₃(L)₄(μ-OH)₂(μ₃-OH)₆(o-val)₂(H₂O)₆]NO₃·7H₂O (1**).** Yield: 0.024 g, 47% (based on Dy³⁺). FT-IR (KBr) cm⁻¹: 3421 (br), 2939 (w), 2837 (w), 1634 (s), 1479 (s), 1447 (s), 1384 (s), 1312 (m), 1289 (m), 1242 (s), 1215 (s), 1168 (w), 1074 (m), 1037 (w), 955 (w), 853 (w), 739 (m), 613 (w), 513 (w). Anal. Calcd. for C₈₀H₁₀₈N₅Dy₃Ni₅O₄₆ (2656.69): C, 36.17; H, 4.10; N, 2.64. Found: C, 36.22; H, 4.01; N, 2.62.

[Ni₅Tb₃(L)₄(μ-OH)₂(μ₃-OH)₆(o-val)₂(H₂O)₆]NO₃·7H₂O (2**).** Yield: 0.027 g, 56 % (based on Tb³⁺). FT-IR (KBr) cm⁻¹: 3423 (br), 2937 (w), 2839 (w), 1633 (s), 1481 (s), 1445 (s), 1384 (s), 1314 (m), 1287 (m), 1243 (s), 1216 (s), 1170 (w), 1071 (m), 1038 (w), 957 (w), 851 (w), 736 (m), 615 (w), 514 (w). Anal. Calcd. for C₈₀H₁₀₈N₅Tb₃Ni₅O₄₆ (2645.96): C, 36.31; H, 4.11; N, 2.65. Found: C, 36.42; H, 4.10; N, 2.66.

[Ni₅Ho₃(L)₄(μ-OH)₂(μ₃-OH)₆(o-val)₂(H₂O)₆]NO₃·7H₂O (3**).** Yield: 0.023 g, 48% (based on Ho³⁺). FT-IR (KBr) cm⁻¹: 3424 (br), 2938 (w), 2836 (w), 1634 (s), 1480 (s), 1446 (s), 1383 (s), 1315 (m), 1290 (m), 1245 (s), 1216 (s), 1169 (w), 1072 (m), 1039 (w), 956 (w), 852 (w), 739 (m), 613 (w), 514 (w). Anal. Calcd. for C₈₀H₁₀₈N₅Ho₃Ni₅O₄₆ (2663.98): C, 36.07; H, 4.09; N, 2.63. Found: C, 36.12; H, 4.10; N, 2.61.

Physical Measurements

Elemental analysis (C, H, N) of the complexes were performed with a Perkin-Elmer model 240C elemental analyser. FT-IR spectral measurements were recorded on KBr disks in a Perkin-Elmer model RX1 FT-IR spectrometer. The purity of the bulk compounds were checked by powder XRD using a BRUKER AXS X-ray diffractometer (40 kV, 20 mA) using Cu-Kα radiation (λ = 1.5418 Å) within 5–50° (2θ) range. The high-resolution HR-MS spectra of the compounds were recorded in electrospray ionization (ESI) mode using a Bruker esquire 3000 plus mass spectrometer. Thermogravimetric analysis (TGA) was carried out by Perkin Elmer Pyris Diamond TG-DTA instrument.



Scheme 1 Synthetic diagram of Ni₅Ln₃ aggregate

Magnetic measurements

Magnetic susceptibility measurements were collected using Quantum Design MPMS[®]3 and MPMS-XL SQUID magnetometers on polycrystalline material in the temperature range 2–300 K under an applied DC magnetic field (H) of 1 kOe. The samples were fixed in eicosane and mounted in a gelatine capsule for the measurements. Magnetization as a function of applied field was investigated in the field and temperature ranges of 0–7 T and 2–10 K, respectively, at a sweep rate of 700 Oe/min. AC test were conducted employing an oscillating magnetic field of 3.5 Oe and frequencies between 1 and 1.5 kHz. DC data were corrected for diamagnetic contributions from the used eicosane and core diamagnetism employing Pascal's constants.

X-ray Crystallography

Single crystal X-ray structural studies of **1**, **2** and **3** were performed on a Bruker SMART APEX-II CCD X-ray diffractometer equipped with a graphite-monochromator Mo- $K\alpha$ ($\lambda = 0.71073$ Å) radiation by the ω scan (width of 0.3° frame⁻¹) at 114 K with a scan rate of 6s per frame. The frames were indexed, integrated and space group was determined by SAINT, SMART and XPREP software.²² The single crystal structures were solved by direct method using SHELXT-(2014/5)²³ and refined by full-matrix least squares technique using SHELXL²⁴ package within Olex2.²⁵ Empirical absorption corrections were performed by a multi-scan method using SADABS program.²⁶ The H atoms were included in idealized positions using refinement with a riding model. Lattice solvent molecules could not be satisfactorily fixed by the present analysis due to heavy disorder. Thus, "PLATON/SQUEEZE" program²⁷ was used to remove those disordered molecules. Crystallographic diagrams were presented using DIAMOND software.²⁸ The crystal data and the cell parameters for compounds **1–3** are summarized in Table S3 in the ESI. Crystallographic data (excluding structure factors) have been deposited with the Cambridge Crystallographic Data Centre as supplementary publications CCDC 1969074, 1969075 and 1969076. These data can also be obtained free of cost at

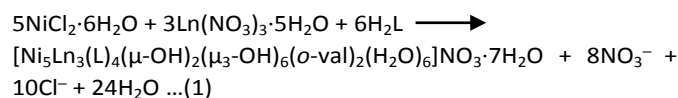
www.ccdc.cam.ac.uk/conts/retrieving.html (or from the Cambridge Crystallographic Data Centre). DOI: 10.1039/D0TD01675F

Result and Discussion

Synthetic Endeavours for Aggregation

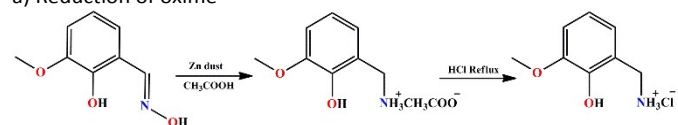
The multisite ditopic ligand H₂L was prepared following the reaction of Scheme 2. The phenol substituted amine was obtained from the reduction of the corresponding oxime following a known procedure.²⁰ Standard Schiff base condensation reaction between resulting amine and the aldehyde provided H₂L in a good yield. The flexible coordination behaviour of the ligand, due to the presence of –CH₂ moiety adjacent to the imine functions, was remarkable for the growth of this heterometallic octanuclear aggregate. Coordination reactivity of pseudo-symmetrical H₂L have been explored by entrapping both the Ln^{III} and Ni^{II} metal ions within the aggregate, with the help of hydroxide groups.

Reaction of NiCl₂·6H₂O and Ln(NO₃)₃·5H₂O salts with H₂L in presence of NEt₃ in MeOH medium under stirring condition lead to [Ni₅Ln₃(L)₄(μ -OH)₂(μ_3 -OH)₆(*o*-val)₂(H₂O)₆]NO₃·7H₂O (Ln = Dy³⁺ (**1**), Tb³⁺ (**2**) and Ho³⁺ (**3**); Scheme 1, eq. 1). Green crystalline powder material was isolated in good yield from the reaction medium when the molar ratio of the individual reactants was optimized at 5:3:6. Room temperature recrystallization of the powdery material from 2:1 v/v MeOH–CHCl₃ mixture, by slow evaporation of the solvents, provided appropriate single crystals.

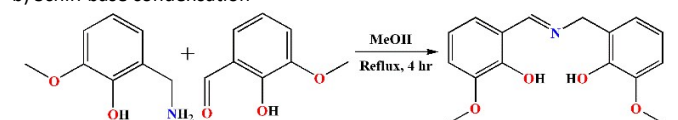


Interestingly the imine bond undergoes hydrolysis reaction, utilized for the growth of the aggregates.²⁹ But despite of several effort we were unable to isolate single crystals of Gd^{III} or Y^{III} analogue from the similar reaction protocol. Complexes **1–3** are characterized by FTIR spectroscopy and the nature of the spectra is familiar for each of the series of the molecule. So only illustrating the spectral characteristics of complex **1** where the band for $\bar{\nu}_{\text{C=N}}$ stretching frequency comes at 1631 cm⁻¹ (Fig. S1 in the ESI). The presence of NO₃⁻ as counter anion also confirms from the peak at 1384 cm⁻¹.³⁰

a) Reduction of oxime



b) Schiff base condensation



Scheme 2 Synthetic flow chart of ligand H₂L

Description of Molecular Structures of Complexes 1–3

The molecular structures of **1–3** in the solid state were determined by single crystal X-ray diffraction. All of them have similar core structure and crystallize in monoclinic $C2/c$ space group. The asymmetric units of **1–3** have been identified as $[\text{Ni}_3\text{Ln}_2(\text{L})_2(o\text{-val})(\mu\text{-OH})(\mu_3\text{-OH})_3(\text{H}_2\text{O})_3]$ (See Fig. S7 in the ESI). For **1** the established molecular formula after the identification of anion and lattice solvent molecules is $[\text{Ni}_5\text{Dy}_3(\text{L})_4(\mu\text{-OH})_2(\mu_3\text{-OH})_6(o\text{-val})_2(\text{H}_2\text{O})_6]\text{NO}_3 \cdot 7\text{H}_2\text{O}$. Complex **1** having Ni_5Dy_3 core is shown in Fig. 2 and the crystal parameters are given in Table S3 in the ESI. Important bond lengths and angles are provided in Tables S4–S5 in the ESI. Due to similar structural type of all three complexes, only structure **1** is described in detail as a representative. The molecular structures, crystal parameters, bond lengths and angles for **2** and **3** are reported in Tables S6–S9 in the electronic supporting Information.

The molecular structure consists of an aggregate of five Ni^{II} and three Dy^{III} ions as a cationic unit associated with single nitrate counter anion to balance the cationic charge. Within these aggregate, four L^{2-} units, each are having two $-\text{OMe}$ groups on both sides, delivering O_4N set of donor atoms. Among these four L^{2-} units, two of them used only one $-\text{OMe}$ group by coordinating Dy1/Dy1^* ions by forming a five membered ring, while the other two have both the $-\text{OMe}$ groups remain pendant. This lead to connectivity patterns 2.12101 and 2.02101³¹ (Fig. S3 in the ESI) to the neighbouring Ni^{II} and Dy^{III} ions. Two $o\text{-val}^-$ units are present as fifth and sixth ligand anions around the four peripheral metal ions (two Ni^{II} and two Dy^{III}) in perpendicular orientation, were obtained from coordination induced imine bond hydrolysis by eliminating the N donor bearing part of the ligand anion. These $o\text{-val}^-$ units were also

utilized to bridge in reverse order of chelation where the six-membered ring is taken up by 4f ions and five-membered rings are formed around the 3d ions³². Apart from bridged $o\text{-val}^-$ units, eight *in situ* solvent derived HO^- groups are used to hold the Ni_5Dy_3 core where six of them function in μ_3 -bridging mode and remaining two are μ -types, resulting mineral like structure of $\text{Ni}_5\text{Dy}_3(\text{OH})_8$ formed from six fused partial cubanes (Fig. 3a). The central butterfly type fused open dicubane $\{\text{NiDy}_3\}$ core is supported by two $\mu_3\text{-HO}^-$ nuclei (See Fig. S8 in the ESI) and the octanuclear structure is grown in four diagonal directions to accommodate four other Ni^{II} centres (Fig. 3a). Within this dicubane core the common NiO_2Dy face bearing 3d and 4f ions has a $\text{Ni3}\cdots\text{Dy2}$ separation of 3.533(4) Å which is longer than the $\text{Ni3}\cdots\text{Dy1}$ distance at 3.343(4) Å and shorter than the $\text{Dy1}\cdots\text{Dy2}$ separation of 3.763(4) Å (Fig. S8 in the ESI). The connectivity established by the six $\mu_3\text{-HO}^-$ (O12 , O12^* , O13 , O13^* , O14 and O14^*) groups and two $\mu\text{-HO}^-$ (O15 and O15^*) groups showed varying Ni-O ; 2.005(5)–2.140(5) Å and Dy-O ; 2.307(5)–2.416(5) Å distances. The angles around central $\mu_3\text{-HO}^-$ nuclei are 104.2(2)°, 99.67(17)° and 105.38(16)° for Ni3-O13-Dy2 , Ni3-O13-Dy1 and Dy1-O13-Dy2 respectively. Within this hexacubane core the shortest intermetallic distance is observed for $\text{Ni2}\cdots\text{Ni3}$ of 3.147(4) Å. The remaining $\text{Ni}\cdots\text{Dy}$ separations are: $\text{Ni1}\cdots\text{Dy1} = 3.421(4)$ Å, $\text{Ni2}\cdots\text{Dy1} = 3.420(5)$ Å and $\text{Ni1}\cdots\text{Dy2} = 3.501(4)$ Å. The hexacubane core is comprised of two $\{\text{Ni}_2\text{Ln}\}$ and four $\{\text{NiLn}_2\}$ face-shared open cubane units (Fig. S11 in the supporting information). The $\mu\text{-HO}^-$ bridges provide narrower Ni2-O15-Ni3 angles of 94.87(18)° compared to the $\mu_3\text{-HO}^-$ bridged Ni2-O14-Ni3 angles of 100.84(18)°. With respect to nature of the ligand types, three distinct types of Ni^{II} centres are present in distorted octahedral O_5N and O_6 coordination environments. Wherein the Ni-N bond distances range within 1.991(5)–2.006(6) Å and Ni-O separations span within 1.981(5)–2.188(5) Å. The centres like Ni1 , Ni1^* , Ni2 and Ni2^* are bound to L^{2-} and hydrolysed ligand, i.e., $o\text{-val}^-$ (Fig. 4a, 4b); whereas Ni3 centre is unique compared to all other metal ion sites, as it is not attached with any ligand donor atom and is held by only six HO^- bridges of two types just discussed (Fig. 4c). Continuous shape measures (CShMs) revealed that, all the three Ni^{II} centres are in distorted octahedron geometry and highest magnitude of deviation from ideal octahedral geometry is observed for Ni1 ($\text{OC-6} = 1.565$, Table S1). Thus with respect to these angular parameters the geometrical distortion is pronounced in case of Ni1 (or Ni1^*) as supported by the CShMs measurements.

All the three Dy^{III} centres present in the aggregate are uniformly eight coordinated. The coordination network for Dy2 is different from Dy1 and Dy1^* . Symmetry matched Dy1 and Dy1^* centres have eight O donors forming the coordination sphere and are arranged from three $\mu_3\text{-HO}^-$, two $\mu\text{-PhO}^-$, one methoxy O, carbonyl O and one terminal water O donors lead to longest Dy-O separation of 2.539(5) Å from O5 and shortest separation of 2.265(5) Å from $\mu\text{-phenoxido O6}$ donor of L^{2-} . The Dy2 centre

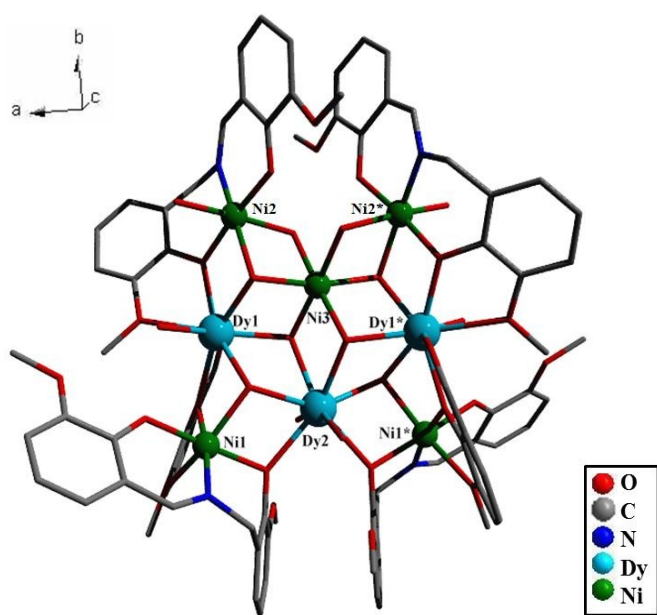


Fig. 2 Molecular structure of complex 1. Counter anion, solvent molecules and H atoms are omitted for clarity.

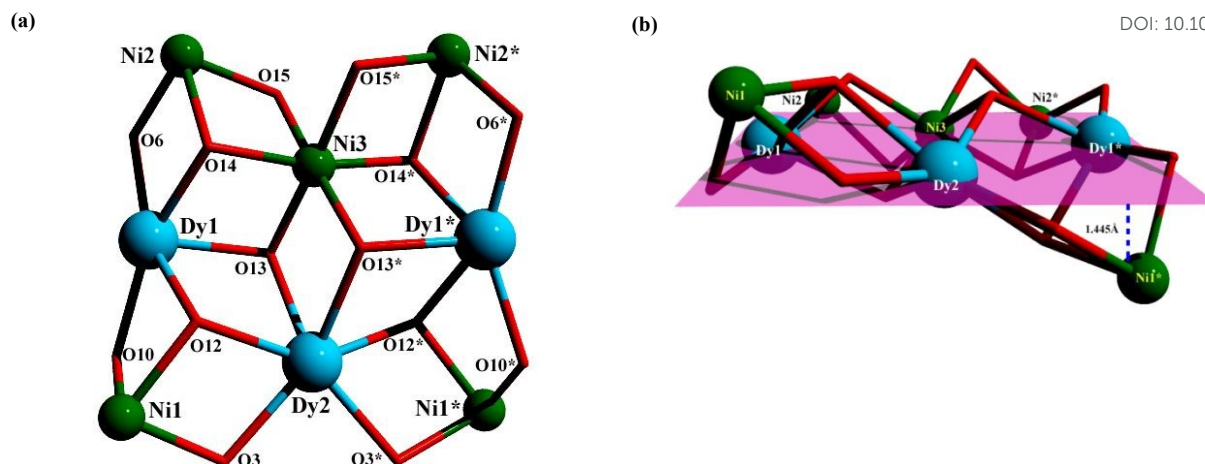


Fig. 3 (a) Core structure of 1 showing the orientation of six partial cubanes; (b) Relative positioning of the metal ions of Ni₅Dy₃ core with respect to the best plane

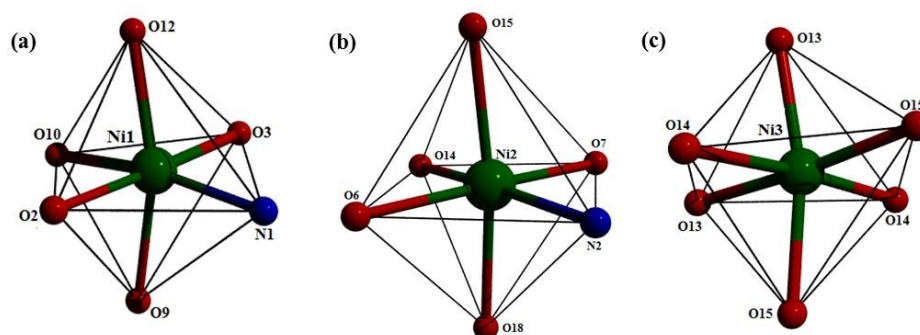


Fig. 4 Varying magnitude of distortion around three Ni^{II} centres (a) Ni1 (Ni1*), (b) Ni2 (Ni2*) and (c) Ni3

is symmetric, having four μ_3 -HO⁻, two μ -phenoxido and two terminal H₂O molecules ensuing in Dy–O separations in 2.347(5)–2.416(5) Å range. According to SHAPE analysis the Dy1 and Dy1* are in distorted trigonal dodecahedron environment (TDD–8 = 0.492, Table S2) and the Dy2 centre adopts a distorted square antiprismatic geometry (SAPR–8 = 0.823, Fig. 5). To estimate the amount of distortion around the SAP geometry of

Table 1 Parameters Involved in SAP Geometry for Dy2

Parameters	Present case	Ideal SAP
φ	40.7°	45°
α	55.2°	54.7°
d_{in}	2.694–2.812	
d_{pp}	2.724–3.142	$d_{pp} = d_{in}$

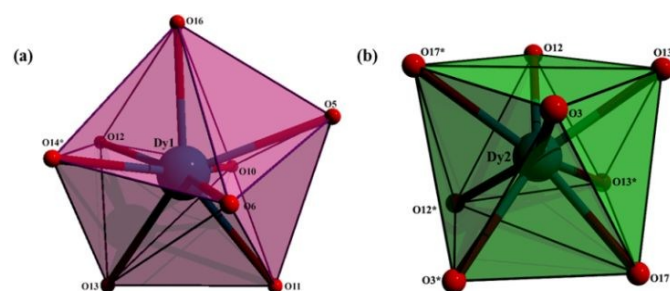


Fig. 5 (a) Distorted trigonal dodecahedron geometry around Dy1 and Dy1*; (b) Distorted square antiprismatic geometry around Dy2

Dy2, we have measured the angle between S8 axis and a Ln–L direction (α), the skew angle (φ), the distance between the square (d_{in}) and the distance between the two parallel squares (d_{pp} , Table 1). The analysis of the data showed that the geometry of Dy2 is noticeably deviated from the ideal SAP and can be considered as compressed square antiprism. The mean plane analysis revealed that all the three Dy^{III} centres and the centrally trapped Ni3 centre of the central dicubane part lies on the same plane. The four Ni^{II} centres at the four corners of this dicubane are placed out of plane with respect to this dicubane motif. The maximum deviation from this plane is observed for Ni1 and Ni1*, which are 1.439 Å away from the mean plane (Fig. 3b). The literature search on known Ni–Ln complexes revealed that only one Ni₅Ln₃ complex is known so far but having a completely different structural type and intermetallic connectivity pattern from the present case (Fig. S17).¹⁷

Mass Spectral Assessment for Complexes 1–3

ESI–MS (+ve mode) analysis of complexes 1–3 were supportive to identify the structural integrity of all the complexes in MeOH solution. The ESI–MS spectra of analytically pure complexes 1–3 were given in the Electronic Supporting Information (Fig. S13–S15). For all the three compounds, identification of the fragments was more or less similar which confirms that the aggregation patterns in all the three cases are same, so taking 1 as specimen for the whole series.

ab initio CASSCF calculations³⁷ performed with OpenMOLCAS software³⁸ on two fragments of Ni_5Dy_3 (see ESI for details) shows that ground state Kramers doublet of Dy1 and Dy1* are characterized by a large axial magnetic anisotropy (Table S10) with a mixture of $m_J = \pm 15/2$ and $\pm 11/2$ states and with a separation of 111 cm^{-1} from the first excited state. Similarly, Dy2 ions was found to have also large axial magnetic anisotropy (Table S11) with a well-defined $m_J = \pm 15/2$ state and with energy separation of 142 cm^{-1} from the first excited state. Thus, all three Dy ions possess properties inevitable for slow relaxation of the magnetization as evidence from calculated magnetization blocking barriers (Fig. S18 and S19, ESI). Conversely, experimental results show no SMM behaviour in the Ni_5Dy_3 complex. Therefore, the impact of mutual dipolar interactions of Dy ions was investigated by POLY_ANISO module of OpenMOLCAS as showed in Fig. 8.

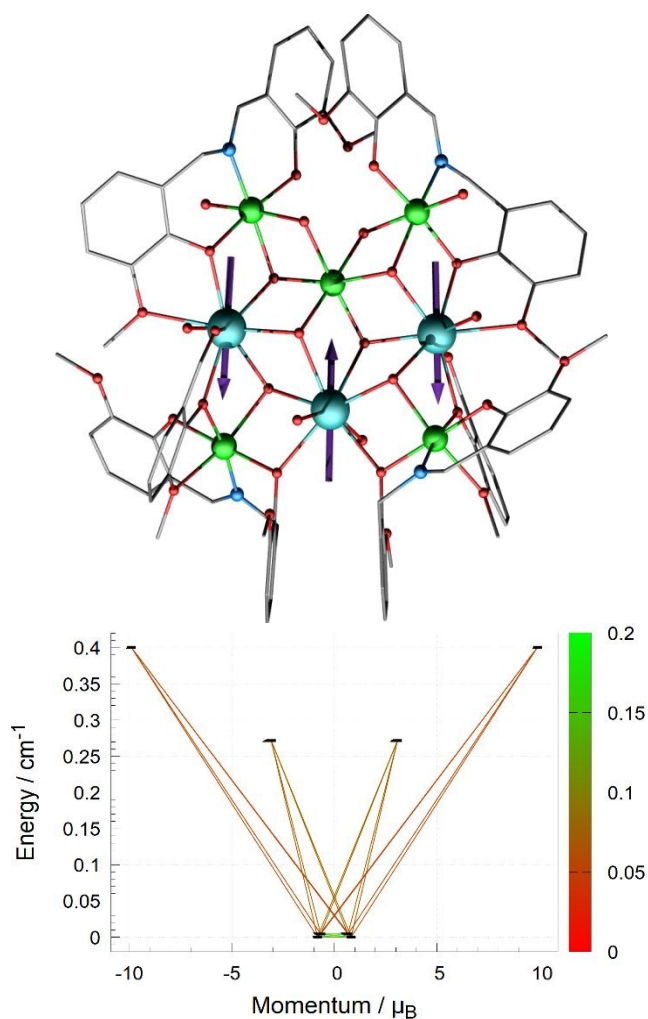


Fig. 8 Top: The molecular structure of Ni_5Dy_3 showing the anisotropy magnetic axes determined by the calculations for Dy1 and Dy2 ions. Color code: Dy, cyan; Ni, green; C, grey; N, blue; O, red. Bottom: Magnetization blocking barrier of Ni_5Dy_3 based on POLY_ANISO calculations taking into account partial calculations for fragments 1 (Dy1) and 2 (Dy2) and dipolar interactions for three lowest Kramers doublets for each Dy ion. The magnetic relaxation path, outlining the blocking barrier, is traced by the red lines, whose intensity scales the transition magnetic dipole matrix elements between the connected multiplet states.

Evidently, the relative orientations of the easy axes of the magnetization degrade magnetic anisotropy properties leading to ground state with very small magnetic productivity and large tendency for the tunnelling of the magnetization. This unfortunate character of dipolar interactions is most likely responsible for lack of SMM features in this polynuclear system. However, also other interactions can contribute to this observation, e.g. $\text{Ni}^{\text{II}}\cdots\text{Dy}^{\text{III}}$ exchange interactions. All this can result in relaxation pathways being highly active, e.g. Raman, QTM, etc., which in turn could diminish the anisotropic character of the Dy^{III} ions and enhance relaxation, as often observed.³⁹

Conclusions

Coordination driven self-assembly reactions have been tested with Schiff base 2-[(2-hydroxy-3-methoxybenzyl)imino]methyl-6-methoxyphenol (H_2L), for the entrapment of $3d$ and $4f$ ions within a single molecular entity. Availability of eight HO^- groups was crucial for the growth of partial hexacubane core topology. The rational design of ligand system, and ligand imine arm hydrolysis could be examined for its aggregation control to assemble Ni_5Ln_3 coordination aggregates, having promise for interesting magnetic properties. Magnetic susceptibility studies show an upsurge at low temperature in the magnetic susceptibility profile of Dy^{3+} and Tb^{3+} analogues, indicative of ferromagnetic interactions whereas for the Ho^{3+} containing complex the interactions is antiferromagnetic in nature. Furthermore, although CASSCF studies predicted SMM behaviour for this multimetallic system, we find fast relaxation within the overall cage structure. Our findings could be due to active relaxation pathways and most likely unfavourable contributions from spatial orientation of the Dy^{III} magnetic axes as suggested from quantitative analysis of CASSCF calculations, thus reducing the overall magnetic anisotropy, thus inducing faster relaxation.

Conflicts of interest

There are no conflicts to declare.

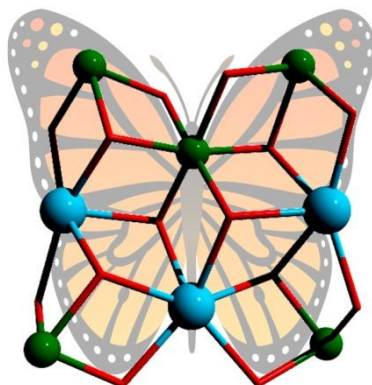
Acknowledgements

A.B. is thankful to DST-INSPIRE for the research fellowship. We acknowledge FIST program of DST, New Delhi for the Single Crystal XRD facility at the Department of Chemistry, IIT Kharagpur. We are thankful to Dr Claire Wilson of University of Glasgow, UK, for modelling the disorder in molecular structure and Prof. Zdeněk Trávníček of Palacký University, Olomouc, Czech Republic, for SHAPE 2.0 calculations of metal ion centre. W.W. thanks the A. v. Humboldt foundation and the ERC grant MoQuOS Nr. 741276. R.H. acknowledges the financial support from institutional sources of the Department of Inorganic Chemistry, Palacký University Olomouc, Czech Republic.

References

- (a) S. K. Langley, D. P. Wielechowski, V. Vieru, N. F. Chilton, B. Moubaraki, B. F. Abrahams, L. F. Chibotaru and K. S. Murray, *Angew. Chem. Int. Ed.*, 2013, **52**, 12014–12019. (b) C. M. Zaleski, E. C. Depperman, J. W. Kampf, M. L. Kirk and V. L. Pecoraro, *Angew. Chem. Int. Ed.*, 2004, **43**, 3912–3914. (c) C. Papatriantafyllopoulou, W. Wernsdorfer, K. A. Abboud and G. Christou, *Inorg. Chem.*, 2011, **50**, 421–423. (d) S. K. Langley, N. F. Chilton, B. Moubaraki and K. S. Murray, *Inorg. Chem. Front.*, 2015, **2**, 867–875. (e) V. Chandrasekhar, A. Dey, S. Das, M. Rouzies and R. Clerac, *Inorg. Chem.*, 2013, **52**, 2588–2598.
- (a) D. Gatteschi, R. Sessoli and J. Villain, Oxford University Press: Oxford, U.K. 2006. (b) D. Gatteschi, *Adv. Mater.*, 1994, **6**, 635–645.
- M. N. Leuenberger and D. Loss, *Nature*, 2001, **410**, 789–793.
- L. Bogani and W. Wernsdorfer, *Nat. Mater.*, 2008, **7**, 179–186.
- (a) A. M. Ako, I. J. Hewitt, V. Mereacre, R. Clerac, W. Wernsdorfer, C. E. Anson and A. K. Powell, *Angew. Chem. Int. Ed.*, 2006, **45**, 4926–4929. (b) Y.-S. Ding, N. F. Chilton, R. E. P. Winpenny and Y.-Z. Zheng, *Angew. Chem. Int. Ed.*, 2016, **55**, 16071–16074.
- D. N. Woodruff, R. E. P. Winpenny and R. A. Layfield, *Chem. Rev.*, 2013, **113**, 5110–5148.
- (a) N. Ishikawa, M. Sugita and W. Wernsdorfer, *J. Am. Chem. Soc.*, 2005, **127**, 3650–3651. (b) F. Ortu, D. Reta, Y.-S. Ding, C. A. P. Goodwin, M. P. Gregson, E. J. L. McInnes, R. E. P. Winpenny, Y.-Z. Zheng, S. T. Liddle, D. P. Mills and N. F. Chilton, *Dalton Trans.*, 2019, **48**, 8541–8545.
- Z. Zhang, Y. Zhang and Z. Zheng, *Struct. Bond.*, 2017, **173**, 1–49.
- (a) S. K. Langley, D. P. Wielechowski, V. Vieru, N. F. Chilton, B. Moubaraki, L. F. Chibotaru and K. S. Murray, *Chem. Sci.*, 2014, **5**, 3246–3256. (b) T. C. Stamatatos, S. J. Teat, W. Wernsdorfer and G. Christou, *Angew. Chem. Int. Ed.*, 2009, **48**, 521–524.
- T. Ishida, R. Watanabe, K. Fujiwara, A. Okazawa, N. Kojima, G. Tanaka, S. Yoshii and H. Nojiri, *Dalton Trans.*, 2012, **41**, 13609–13619.
- J. Rinck, G. Novitchi, W. V. D. Heuvel, L. Ungur, Y. Lan, W. Wernsdorfer, C. E. Anson, L. F. Chibotaru and A. K. Powell, *Angew. Chem. Int. Ed.*, 2010, **49**, 7583–7587.
- (a) G. Karotsis, M. Evangelisti, S. J. Dalgarno and E. K. Brechin, *Angew. Chem. Int. Ed.*, 2009, **48**, 9928–9931. (b) A. Mishra, W. Wernsdorfer, K. A. Abboud and G. Christou, *J. Am. Chem. Soc.*, 2004, **126**, 15648–15649. (c) T. Shiga, T. Onuki, T. Matsumoto, H. Nojiri, G. N. Newton, N. Hoshino and H. Oshio, *Chem. Commun.*, 2009, 3568–3570.
- (a) S. Chen, V. Mereacre, G. E. Kostakis, C. E. Anson and A. K. Powell, *Inorg. Chem. Front.*, 2017, **4**, 927–934. (b) F. Pointillart, K. Bernot, R. Sessoli and D. Gatteschi, *Chem. Eur. J.*, 2007, **13**, 1602–1609.
- Y.-Z. Zheng, M. Evangelisti, F. Tuna and R. E. P. Winpenny, *J. Am. Chem. Soc.*, 2012, **134**, 1057–1065.
- A. Worrell, D. Sun, J. Mayans, C. Lampropoulos, A. Escuer and T. C. Stamatatos, *Inorg. Chem.*, 2018, **57**, 13944–13952.
- (a) N. Ahmed, C. Das, S. Vaidya, S. K. Langley, K. S. Murray and M. Shanmugam, *Chem. Eur. J.*, 2014, **20**, 14235–14239. (b) A. Bhanja, R. Herchel, Z. Travnicek and D. Ray, *Inorg. Chem.*, 2019, **58**, 12184–12198.
- H. Wang, H. Ke, S.Y. Lin, Y. Guo, L. Zhao, J. Tang and Y. -H. Li, *Dalton Trans.*, 2013, **42**, 5298–5303.
- A. K. Ghosh, M. Shatruck, V. Bertolasi, K. Pramanik and D. Ray, *Inorg. Chem.*, 2013, **52**, 13894–13903.
- B. S. Furniss, A. J. Hannaford, P. W. G. Smith and A. R. Tatchell, *Vogel's Text book of Practical Organic Chemistry*, 5th ed.; ELBS, Longman: London, U.K. 1989.
- I. Zagol-Ikapitte, V. Amarnath, M. Bala, L. J. Roberts, J. A. Oates and O. Boutaud, *Chem. Res. Toxicol.*, 2010, **23**, 240–250.
- J. Zhang, H. Zhang, Y. Chen, X. Zhang, Y. Li, W. Liu and Y. Dong, *Dalton Trans.*, 2016, **45**, 16463–16470. DOI: 10.1039/D0DT01675F
- SAINT, SMART and XPREP*, Siemens Analytical X-ray Instruments Inc.: Madison, WI, 1995.
- G. M. Sheldrick, *Acta Crystallogr., Sect. A: Found. Adv.* 2015, **71**, 3–8.
- G. M. Sheldrick, *Acta Crystallogr., Sect. C: Struct. Chem.* 2015, **71**, 3–8.
- O. V. Dolomanov, L. J. Bourhis, R. J. Gildea, J. A. K. Howard and H. J. Puschmann, *J. Appl. Crystallogr.*, 2009, **42**, 339–341.
- G. M. Sheldrick, *SADABS Software for Empirical Absorption Correction*, University of Göttingen, Institute für Anorganische Chemieder Universität, Göttingen, Germany, 1999–2003.
- A. L. Spek, *Acta Crystallogr., Sect. C: Struct. Chem.* 2015, **71**, 9–18.
- DIAMOND, Visual Crystal Structure Information System, version 3.1, Crystal Impact: Bonn, Germany, 2004.
- M. Pait, A. Bauzá, A. Frontera, E. Colacio and D. Ray, *Inorg. Chem.*, 2015, **54**, 4709–4723.
- K. Nakamoto, *Infrared Spectra of Inorganic and Coordination Compounds*, 4th ed. Wiley Interscience. New York, 1986.
- R. A. Coxall, S. G. Harris, D. K. Henderson, S. Parsons, P. A. Tasker and R. E. P. Winpenny, *J. Chem. Soc. Dalton Trans.*, 2000, 2349–2356.
- J.-P. Costes, F. Dahan, L. Vendier, S. Shova, G. Lorusso, and M. Evangelisti, *Dalton Trans.*, 2018, **47**, 1106–1116.
- (a) J. Paulovič, F. Cimpoesu, M. Ferbinteanu and K. Hirao, *J. Am. Chem. Soc.*, 2004, **126**, 3321–3331. (b) R. E. P. Winpenny, *Chem. Soc. Rev.*, 1998, **27**, 447–452. (c) E. Moreno-Pineda, N. F. Chilton, F. Tuna, R. E. P. Winpenny and E. J. L. McInnes, *Inorg. Chem.*, 2015, **54**, 5930–5941.
- E. Moreno-Pineda, Y. Lan, O. Fuhr, W. Wernsdorfer and M. Ruben, *Inorg. Chem.*, 2018, **57**, 9873–9879.
- (a) M. A. Halcrow, J. Sun, J. C. Huffman and G. Christou, *Inorg. Chem.*, 1995, **34**, 4167–4177. (b) R. Herchel, I. Nemeč, M. Machata and Z. Travnicek, *Dalton Trans.*, 2016, **45**, 18622–18634.
- L. R. Piquera and E. C. Sañudo, *Dalton Trans.*, 2015, **44**, 8771–8780.
- (a) P. E. M. Siegbahn, J. Almlöf, A. Heiberg and B. O. Roos, *J. Chem. Phys.*, 1981, **74**, 2384–2396. (b) J. Olsen, B. O. Roos, P. Jørgensen and H. J. A. Jensen, *J. Chem. Phys.*, 1988, **89**, 2185–2192. (c) P. A. Malmqvist, B. O. Roos and B. Schimmelpfennig, *Chem. Phys. Lett.*, 2002, **357**, 230–240. (d) L. Ungur and L. F. Chibotaru, *Chem. Eur. J.*, 2017, **23**, 3708–3718. (e) L. F. Chibotaru and L. Ungur, *J. Chem. Phys.*, 2012, **137**, 064112.
- I. Fdez. Galván, M. Vacher, A. Alavi, C. Angeli, F. Aquilante, J. Autschbach, J. J. Bao, S. I. Bokarev, N. A. Bogdanov, R. K. Carlson, L. F. Chibotaru, J. Creutzberg, N. Dattani, M. G. Delcey, S. S. Dong, A. Dreuw, L. Freitag, L. M. Frutos, L. Gagliardi, F. Gendron, A. Giussani, L. González, G. Grell, M. Guo, C. E. Hoyer, M. Johansson, S. Keller, S. Knecht, G. Kovačević, E. Källman, G. Li Manni, M. Lundberg, Y. Ma, S. Mai, J. P. Malhado, P. Å. Malmqvist, P. Marquetand, S. A. Mewes, J. Norell, M. Olivucci, M. Oettel, Q. M. Phung, K. Pierloot, F. Plasser, M. Reiher, A. M. Sand, I. Schapiro, P. Sharma, C. J. Stein, L. K. Sørensen, D. G. Truhlar, M. Ugandi, L. Ungur, A. Valentini, S. Vancoillie, V. Veryazov, O. Weser, T. A. Wesolowski, P.-O. Widmark, S. Wouters, A. Zech, J. P. Zobel and R. Lindh, *J. Chem. Theory Comput.*, 2019, **15**, 5925–5964.
- (a) R. J. Blagg, L. Ungur, F. Tuna, J. Speak, P. Comar, D. Collision, W. Wernsdorfer, E. J. L. McInnes, L. F. Chibotaru and R. E. P. Winpenny, *Nat. Chem.*, 2013, **5**, 673–678. (b) F. Habib, P.-H. Lin, J. Long, I. Korobkov, W. Wernsdorfer and M. Murugesu, *J. Am. Chem. Soc.*, 2011, **133**, 8830–8833. (c) K. R. Meihaus, J. D. Rinehart and J. R. Long, *Inorg. Chem.*, 2011, **50**, 8484–8489.

Synopsis. Octanuclear $\text{Ni}^{\text{II}}_5\text{Ln}^{\text{III}}_3$ complexes were obtained with ligand H_2L . View Article Online
DOI: 10.1039/C9DT01675F shows ferromagnetic interactions for Ni_5Dy_3 and Ni_5Tb_3 while antiferromagnetic in Ni_5Ho_3 .



[For Table of Contents Only](#)